ELSEVIER

Wall effects on the flow of viscoelastic fluids around a circular cylinder

P.Y. Huang, J. Feng *

Department of Aerospace Engineering and Mechanics and The Minnesota Supercomputer Institute, University of Minnesota, Minneapolis, MN 55455, USA

Abstract

In this paper, we use numerical simulations to study two-dimensional steady flows of a viscoelastic fluid past a circular cylinder confined by two parallel walls. The drag on the cylinder and the velocity profile in its wake are investigated as functions of the wall blockage and properties of the fluid. The interplay among wall effects, elasticity, shear thinning and inertia is examined in detail. Results show that wall proximity shortens the wake and increase the drag, and this effect is reduced by fluid elasticity. For weak wall blockage, elasticity increases the drag and lengthens the wake for Reynolds number $Re = 0.1 - 10$. For stronger blockage this trend is reversed. Shear thinning decreases the drag and shortens the wake for all Reynolds numbers, Weissenberg numbers and blockage ratios we have tested. A negative wake appears for the strongest wall blockage.

Keywords: Circular cylinder; Flow; Viscoelastic fluids; Wall effects

1. Introduction

Walters and Tanner [1] have reviewed the theoretical and experimental works on flow past a sphere with or without wall confinement. Almost all the results mentioned in their paper are for creeping flows. The following tentative picture has emerged for motion in unbounded domains. (i) For a Boger fluid, the drag is not affected by elasticity when the Weissenberg number $We < 0.1$; the drag is reduced

---

* Corresponding author.

when $0.1 < We < 1$. A plateau seems to exist in $1 < We < 2$, after which the drag increases with We. (ii) The streamlines around the sphere are slightly shifted downstream at small We but shifted upstream at higher We. There are exceptions to the above "rules". For instance, Chmielewski et al. [2] obtained a virtually constant drag for a polybutene-based Boger fluid up to $We = 0.2$. Van de Brule and Gheissary [3] reported that the settling of a sphere in a viscoelastic fluid is always slower than that in a Newtonian fluid of comparable viscosity; this difference in fall velocity increases with the Weissenberg number in the range tested, which appears to be roughly $0.01 < We < 0.2$.

Wall effects are studied on the flow past a sphere moving along the axis of a circular cylinder. For viscoelastic fluids without shear thinning, only creeping flows have been studied. The ratio between the radius of the sphere and the cylinder is denoted by β. For $\beta < 0.15$, elasticity does not interfere with the wall effect and Newtonian results (e.g., Faxén's formula) can be used [2,4,5]. For stronger blockage, experiments [6–9] and calculations [5,10] agree that the wall effect is reduced by elasticity, but there is no quantitative agreement as to the magnitude of this reduction. In particular, Chhabra and Uhlherr [8] reported that the elastic effect is so strong as to virtually eliminate the wall effect! Shear thinning reduces the wall effect for purely viscous and viscoelastic fluids, at all Reynolds number [9,11]. Recently, Jones et al. [12] presented some new data on the drag coefficient for a sphere in a falling-ball apparatus.

The flow of a viscoelastic liquid past a circular cylinder in an infinite domain has been studied extensively [13]. Two distinctive regimes exist, depending on the Mach number of the flow. If the relative velocity of the liquid with respect to the cylinder is larger than the shear wave speed of the liquid, a shock wave of vorticity forms in front of the cylinder [14]. Between the shock and the solid surface is a layer of relatively stagnant fluid, which accounts for the increased drag and decreased heat transfer on the cylinder [15]. The hyperbolic nature of this regime was first recognized by Ultman and Denn [16]. Existence of the shock wave was later confirmed by numerical simulations [17,18] and LDV measurements [19].

Flows associated with small Reynolds numbers and Weissenberg numbers are amenable to perturbation analysis [16,20]. More recently, numerical computation was employed to treat stronger flows around a cylinder in an unbounded domain [21]. Experiments have been carried out for different ranges of Re and We [22–24]. At small Re and We, there is a downstream shift in the streamlines and the drag is reduced as compared with the Newtonian value; at high Re and We, the streamlines shift upstream and the drag is increased by elasticity. Again, there is considerable inconsistency among data from different sources, especially about the shifting of streamlines. In fact, Townsend [21] concluded, after summarizing experimental and theoretical results available at that time, that there is no consistent trend in the shifting of streamlines. For example, Ultman and Denn [16] report a significant upstream shift in streamlines in a very weak flow ($Re = 2 \times 10^{-4}$, $We = 3.2 \times 10^{-3}$), while Broadbent and Mena [22] and Carew and Townsend [25] observed no discernible change in the streamlines due to viscoelasticity.

There is no systematic study of the wall effects on flow around cylinders in a bounded domain. Dhahir and Walters [26] measured the force on a cylinder placed in a channel flow. The undisturbed velocity profile is fully developed and only one blockage ratio ($\beta = 0.6$) is studied. For a Boger fluid and a shear thinning polyacrylamide solution, the drag on the cylinder is reduced by viscoelasticity. A lateral force arises when the cylinder is in an eccentric position, which tends to push the cylinder towards the closer wall. These results were later corroborated by the numerical simulations of Carew and Townsend [25]. Recently, McKinley et al. [13] used LDV to measure the flow around a cylinder fixed in the middle of a channel. A downstream shift in the streamlines was reported. Baaijens et al. [27] measured the stress field near a cylinder in a channel flow.

In this paper we will study wall effects on the flow around a cylinder by numerical simulations using POLYFLOW. The influences of elasticity and shear thinning will be examined. Because of the high-We difficulty in convergence, most of the results fall into the subsonic regime and we will not attempt to explore flow features related to hyperbolicity. The cylinder is fixed in space and immersed in a flow that is otherwise uniform. Two bounding walls are moving with the same uniform velocity. This is the two dimensional analog of the falling-ball viscometer, which has been a benchmark problem for viscoelastic simulations.

The present problem is interesting to us primarily because it provides the fundamental information about the wall effects in two dimensions, which has been missing in the literature. This geometry has been related to certain procedures in polymer processing and especially flows through porous media [13]. Also, it is the basis for two-dimensional dynamic simulations of the motion of solid bodies in a viscoelastic fluid.

2. Formulation of the problem

The geometry of the problem is shown in Fig. 1. The equations of motion are

$$\begin{cases} \nabla \cdot \boldsymbol{u} = 0, \\ \rho\left(\dfrac{\partial \boldsymbol{u}}{\partial t} + \boldsymbol{u} \cdot \nabla \boldsymbol{u}\right) = -\nabla p + \nabla \cdot \boldsymbol{T}. \end{cases}$$

The constitutive model used in this work is the Oldroyd-B model with a shear-rate dependent viscosity; it can also be seen as a White–Metzner model with an added viscous component:

$$\boldsymbol{T} + \lambda_1 \overset{\triangle}{\boldsymbol{T}} = 2\eta(\dot{\gamma})(\boldsymbol{D} + \lambda_2 \overset{\triangle}{\boldsymbol{D}}),$$

where $\boldsymbol{D} = (\nabla \boldsymbol{u} + \nabla \boldsymbol{u}^{\mathrm{T}})/2$ is the strain-rate tensor; λ_1 and λ_2 are constant relaxation and retardation times. The triangle denotes the upper-convected time-derivative:

$$\overset{\triangle}{\boldsymbol{T}} = \frac{\partial \boldsymbol{T}}{\partial t} + \boldsymbol{u} \cdot \nabla \boldsymbol{T} - (\nabla \boldsymbol{u}) \cdot \boldsymbol{T} - \boldsymbol{T} \cdot (\nabla \boldsymbol{u})^{\mathrm{T}}.$$

The Carreau–Bird viscosity law is adopted:

$$\frac{\eta - \eta_\infty}{\eta - \eta_0} = [1 + (\lambda_3 \dot\gamma)^2]^{(n-1)/2}.$$

The boundary conditions are:

$u = -U$, $v = 0$, $T = 0$ at $x = \infty$ (inflow);

$u = -U$, $v = 0$ at $y = 0$ and L (side walls);

$u = -U$, $v = 0$ at $x = -\infty$ (outflow);

$u = 0$, $v = 0$ on the surface of the cylinder.

In actual computation, the domain is taken to be a rectangle that extends a certain distance upstream and downstream of the cylinder. Then the outlet condition is relaxed to vanishing forces in both directions.

The most important dimensionless groups include the Reynolds number $Re = \rho U d / \eta_0$ which indicates the magnitude of the inertial effect, the Weissenberg number $We = 2\lambda_1 U / d$ which represents the elastic effect, the power index n which represents the degree of shear thinning and the blockage ratio $\beta = d/L$ which represents the wall effect. Other parameters in the problem, λ_2/λ_1, λ_3/λ_1 and η_∞/η_0, have less physical significance and are not varied systematically in the computations. We will be primarily interested in the drag coefficient of the cylinder:

$$C_d = \frac{\text{Drag per unit length}}{\frac{1}{2}\rho U^2 \cdot d}$$

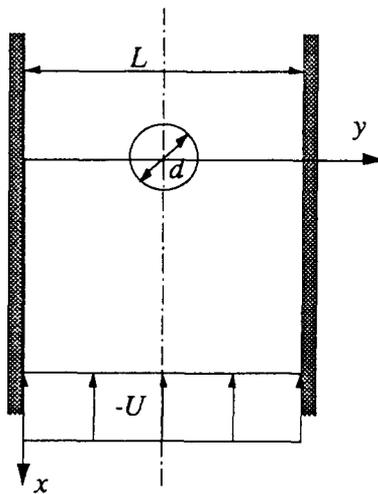and the velocity field around it, especially in the wake.
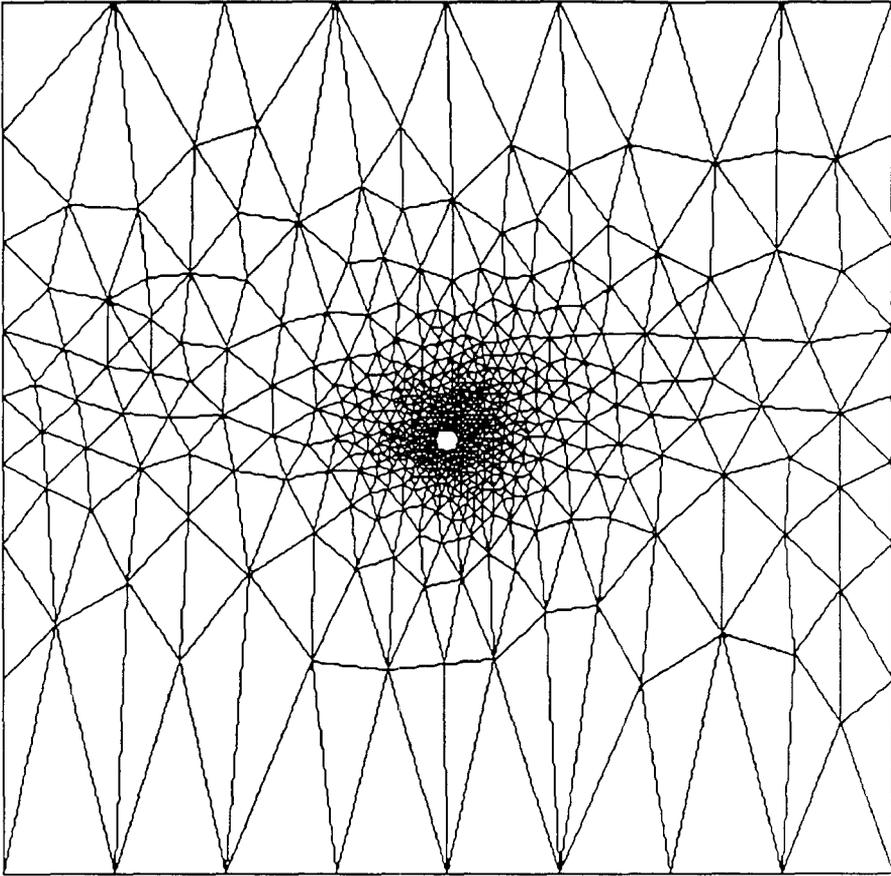

Fig. 1. Geometry of the problem.

Fig. 2(i).

The solution is obtained by using POLYFLOW-3, an updated version of the viscoelastic package developed by Prof. M.J. Crochet and co-workers. This code employs a finite element method with the elastic-viscous stress split scheme (EVSS). The EVSS scheme has been described by Rapajopalan et al. [28] and the POLYFLOW algorithm by Legat and Marchal [29] and Debae et al. [30]. In our simulations we use an unstructured mesh with triangular elements. A typical mesh used for $\beta = 0.025$ is shown in Fig. 2. Mesh refinement has been done systematically to ensure convergence. For instance, refining the mesh in Fig. 2 to 4114 nodes and 2026 elements results in a 0.74% difference in the drag at $Re = 1$ and $We = 1$. For wider channels, we use up to 6844 nodes and 3372 elements.

The code fails to converge when the Weissenberg number exceeds a limiting value. This value also depends on the Reynolds number, the blockage ratio and the degree of shear thinning; higher We can be reached for smaller Re, smaller β and milder shear thinning. As an example, We obtained convergent results up to $We = 2.5$ at $Re = 1$, $\beta = 0.1$ and $n = 1$, but failed with $We = 3$.

3. Results and discussions

As mentioned before, the present problem involves the combined effects of inertia, elasticity, shear thinning and blockage. To characterize each factor separately, we approach the problem in four steps: (1) the flow of a Newtonian fluid around a cylinder in a bounded domain; (2) the flow of a constant-viscosity elastic fluid around a cylinder in an unbound domain; (3) the flow of a shear thinning elastic fluid around a cylinder in an unbound domain and (4) the flow of a shear thinning elastic fluid around a cylinder in a bounded domain. Limited data relevant to (1) and (2) can be found in the literature. The flow of a Newtonian fluid around a cylinder in a bounded domain has been studied at vanishing Re and extremely large Re (over 10^4). The former allows perturbation solution (see Happel and Brenner [31], p. 344); the latter has been studied in wind tunnels by civil engineers
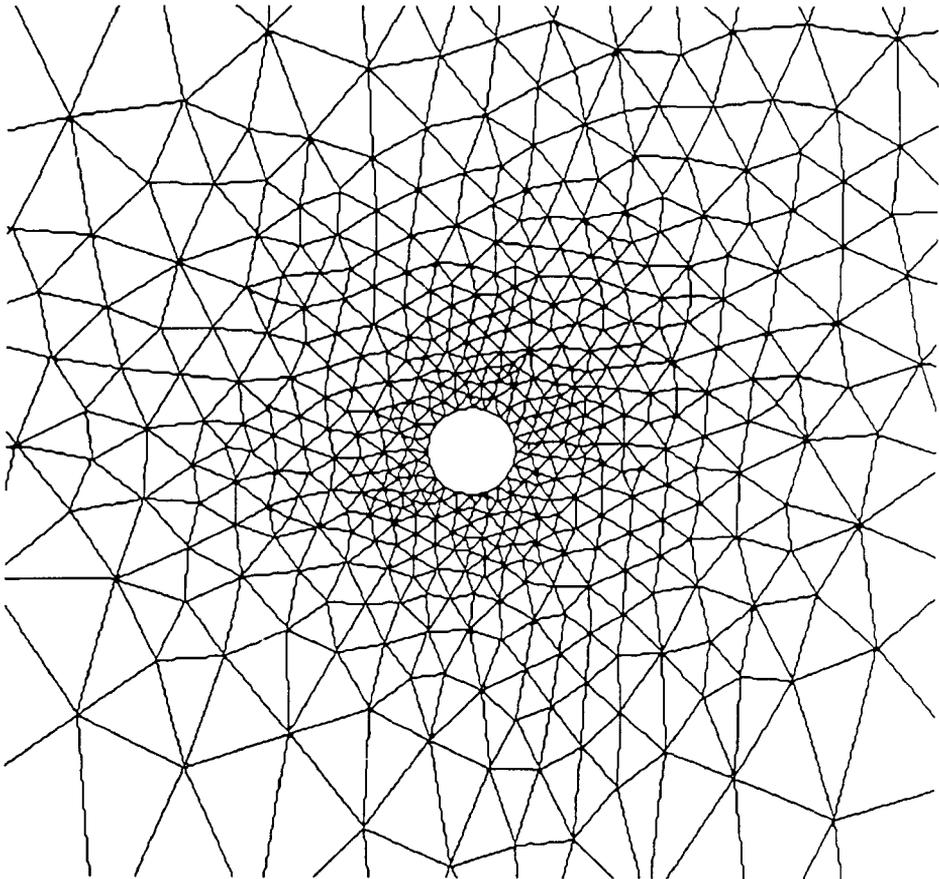

Fig. 2(ii).

Fig. 2. A typical mesh used for $\beta = 0.025$. It has 2420 nodes and 1184 elements; (iii) shows details of the mesh near the cylinder.

because of its significance in wind engineering [32]. No results were found in the intermediate Re range, say, $0.1 < Re < 100$, which is of interest here. For the second sub-problem, perturbation results exist which are valid in the limit of vanishing Re and We. Townsend [21] presented a numerical simulation at non-vanishing Re and We. But the emphasis of that paper was on rotating cylinders and only two data points ($Re = 5$ and 10, $We = 0.6$) were reported for stationary cylinders. In particular, no data were presented for the small-Re regime, in which the drag is said to be decreased by elasticity.

To approximate an unbounded domain in our numerical simulation, we use an extremely wide channel ($L = 400d$) and then relax the boundary conditions on side walls to vanishing forces. The computation domain is extended up to $150d$ upstream of the cylinder and $250d$ downstream.

3.1. Wall effects for a Newtonian fluid

First let us consider the flow of a Newtonian fluid around a cylinder fixed between two parallel walls. This is equivalent to the steady settling of a cylinder through a quiescent fluid in a vertical channel [33]. For an "unbounded" domain ($L = 400d$), the Newtonian drag on the cylinder is compared with the 'standard drag' of Sucker and Brauer [34]. Our drag coefficient is 3.0% larger than the standard drag at $Re = 10$, 4.9% larger at $Re = 1$ and 3.2% smaller at $Re = 0.1$. Using wider channels or finer mesh reduces the discrepancy at higher computational cost. We will consider $L = 400d$ the case with zero wall effect, and will use it as a starting point for studying wall effects.

As shown in Fig. 3, blockage increases the drag coefficient C_d at all Reynolds numbers. The effect is more conspicuous at smaller Re when the disturbance of the cylinder is felt farther away. For $\beta = 0.5$, the drag coefficient is increased by 7.4 times (as compared to the drag at $\beta = 0$) at $Re = 10$ and 33.6 times at $Re = 0.1$. The Faxén formula (see Happel and Brenner [31], p. 344), when applied at $Re = 0.1$ and $0.01 < \beta < 0.33$, gives very good agreement with our computation.

The velocity distribution along the centerline of the flow is shown in Fig. 4 for a cylinder in an unbounded domain. There is a remarkable asymmetry between the upstream and downstream of the cylinder, consistent with Oseen's solution. Increasing the Reynolds number shortens the wake behind the cylinder. Fig. 5 shows the variation of the velocity along the centerline at different blockage ratios. As the blockage ratio β increases, the wake gets shorter and so is the region of disturbance ahead of the cylinder; the velocity distribution becomes more fore-aft symmetric.

3.2. Effects of elasticity in an infinite domain

We consider the flow of an Oldroyd-B fluid with constant viscosity around the cylinder in an infinite domain. The ratio between the retardation time and the relaxation time is fixed at $\lambda_2/\lambda_1 = 0.125$. The effect of We on the drag coefficient C_d at three different Reynolds numbers in shown in Fig. 6. At $Re = 0.1$, there is a slight increase in C_d (only 0.44%) as We increase from 0 to 2. For $Re = 1$, the increase in the drag
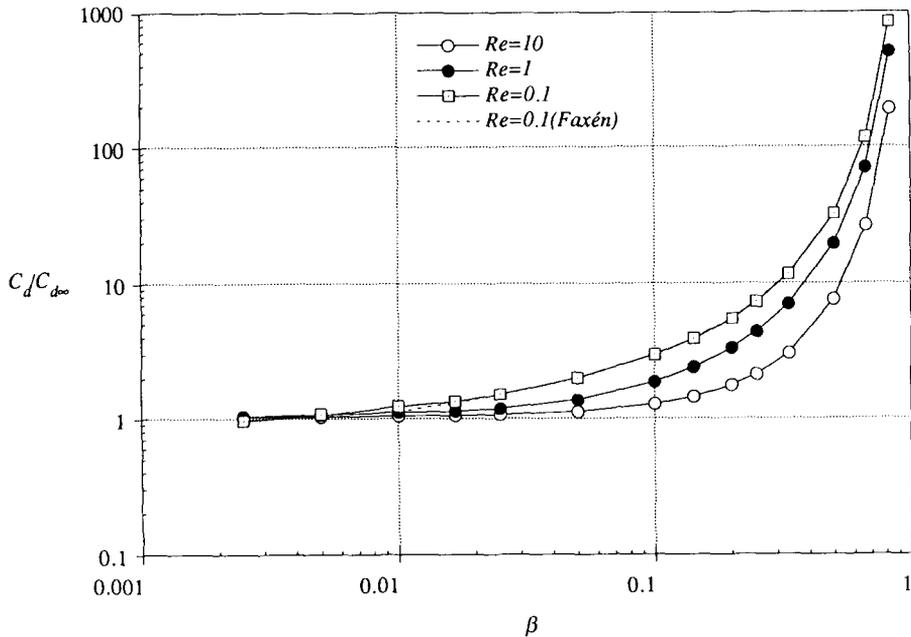
Fig. 3. Wall effects on the drag coefficient of a cylinder in a Newtonian flow. $C_{d\infty}$ is the standard drag coefficient for an infinite domain [34].

is more appreciable. In the case of $Re = 10$, the increase is even larger (up to 9%) as We increases from 0 to 1. Also shown is a data point of Hu and Joseph [18] obtained from a finite-volume method; the discrepancy between the two studies is 0.2%.

The drag increase at $Re = 1$ and 10 agrees with the trend established in previous studies. For vanishing Re, perturbation theory shows that the first order effect of We on C_d is zero; at second order there is a negative correction term which implies a slight drag reduction at small We. This drag reduction is not present in our results at $Re = 0.1$. This may be because the second-order drag reduction is too small for the resolution of our numerical method. Another possibility is that $Re = 0.1$ is not small enough for the perturbation theory to apply. Broadbent and Mena [22] reported drag reduction of up to 30% for the flow of a 2% aqueous polyacrylamide solution around a cylinder at $Re \approx 0.1$ and $We \approx 0.01$, which represents the upper bound of the range in which the drag reduction is proportional to We^2. The magnitude of drag reduction, however, appears suspiciously large. We feel that these data are not reliable because in the experiments, the wall confinement was corrected using a factor deduced from Newtonian flows. It is known that for a sphere in a cylinder tube, the wall effect is much reduced by elasticity, especially at large blockage ratio. Thus, using the Newtonian wall correction would yield much smaller drag value. In fact, Broadbent and Mena [22] admitted that they "look only for qualitative results" because of the rough correction of wall effects. Therefore, their tremendous drag reduction does not invalidate our results of a slightly increasing drag at $Re = 0.1$.

Fig. 7 shows the effects of elasticity on the wake of the cylinder at three Reynolds numbers. There is a downstream shift in the streamlnes; the wake is lengthened by the presence of elasticity and the velocity recovery is slower behind the cylinder. This effect gets stronger as the Reynolds number is increased from $Re = 0.1$ to $Re = 10$. As the Weissenberg number is relatively small, the downstream shift appears to be consistent with the general trend established in the literature [13]. In particular, Chilcott and Rallison [35] simulated the unbounded flow around cylinders and spheres using a constitutive equation for dumbbells with finite extensibility. The wake is longer than that of a Newtonian flow. Using the Maxwell model for a sphere in a tube, Zheng et al. [36] obtained the same wake lengthening, but ascribed it to wall proximity. The present results, along with Chilcott and Rallison [35], confirm that this is an elastic effect. The wall proximity, as to be seen in Section 3.4, actually tends to shorten the wake.

3.3. Effect of shear thinning in an infinite domain

By using the Carreau–Bird law, we can achieve various degrees of shear thinning by varying the power-law index n. Other parameters are $\lambda_3/\lambda_1 = 0.1$ and $\eta_\prime / \eta_0 = 0.1$. For relatively large Weissenberg numbers, as n gets smaller and shear thinning gets more pronounced, numerical convergence becomes more difficult to achieve. Fig. 8 shows the effect of shear thinning on the drag coefficient. The drag
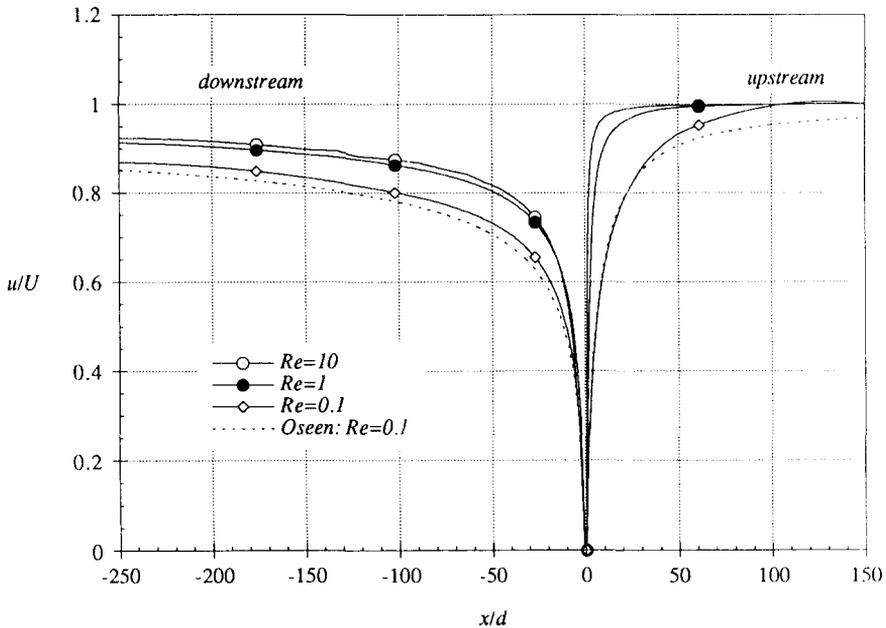

Fig. 4. Velocity distribution on the centerline of an unbounded flow field around a cylinder. Oseen's approximate solution at $Re = 0.1$ is also shown for comparison.
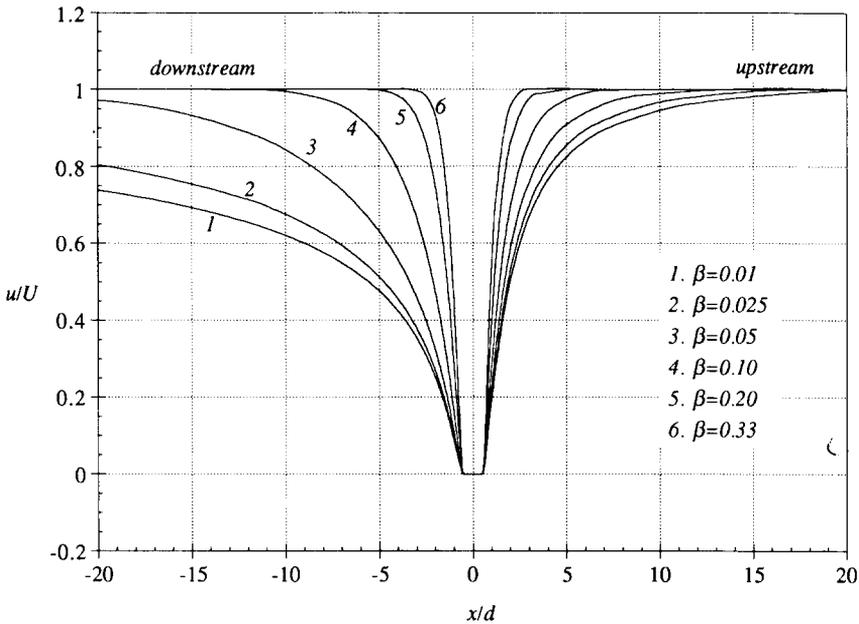
Fig. 5. Wall effects on the velocity distribution along the centerline of the flow field. $Re = 1$.

reduction due to shear thinning is distinctive but small in magnitude, about 4.4% as n goes from 1 to 0.2.

Shear thinning appears to shorten the wake behind the cylinder and cause an upstream shift in the streamlines (Fig. 9). A similar trend was obtained by Zheng et al. [37] for a sphere-in-a-tube geometry using the Phan-Thien–Tanner model. This effect is opposite to that of elasticity. For $n = 0.6$ and 0.2, shear-thinning overwhelms elasticity and the streamlines are shifted upstream as compared to the Newtonian wake.

3.4. Wall effects for a viscoelastic fluid

Our simulations indicate that wall effects are reduced by elasticity and shear thinning. Fig. 10 compares wall effects on the drag coefficients for a Newtonian fluid and a constant-viscosity Oldroyd-B fluids at two Weissenberg numbers. In an unbounded domain, C_d is larger for higher We (compare Fig. 6). As the blockage ratio β increases, C_d incerases both for the Newtonian fluid and for the viscoelastic fluid. For the Oldroyd-B fluid, this wall-induced drag increase is not as steep as for the Newtonian fluid, and the latter catches up with the former at $\beta \approx 0.1$ (Fig. 10(a)). At even larger β, the Newtonian drag is larger than the drag for the Oldroyd-B fluids and the difference grows with β (Fig. 10(b)). Thus, the wall effect is suppressed by viscoelasticity. One may also say that the blockage reverses the effect of elasticity on the drag coefficient. Shear thinning tends to aggravate this trend. Fig. 11 shows that with shear thinning, the drag coefficient becomes increasingly smaller than that for the Oldroyd-B fluid without shear thinning.

These numerical results are consistent with experimental observations of wall effects on cylinders and spheres. Dhahir and Walters [26] studied a channel flow of a viscoelastic fluid past a cylinder confined by parallel walls. For $\beta = 0.6$, they obtained a drag that is smaller than that for a Newtonian fluid. For falling spheres in a tube, it has also been established that elasticity and shear thinning both reduce effects of blockage. For instance, Bisgaard [7] reported that the wall correction factor $C_d/C_{d\infty}$ is a rapidly decreasing function of the Weissenberg number. Mena et al. [9] noted that shear-thinning suppresses the wall effects greatly.

The confinement of side walls shortens the wake behind the cylinder and makes the upstream and downstream velocity variations more symmetric (Fig. 12). This is quite similar to the wall effect on the Newtonian wake (compare Fig. 5). Bush [38] obtained the same effect for an axisymmetric flow past a sphere in the center of a tube.

To reveal the viscoelastic effects on the flow in the presence of wall confinement, we compare the Newtonian wake and the wake for an Oldroyd-B fluid at various blockage ratios (Fig. 13). For small values of β, as for an unbound flow, the viscoelastic wake is longer than the Newtonian wake (e.g., $\beta = 0.05$). This is also when the cylinder experiences a larger drag in a viscoelastic fluid (compare Fig. 10(a)). At $\beta = 0.1$, the two velocity profiles almost coincide. Interestingly, this is also when the drag coefficients coincide. Further increasing β continues to shorten the viscoelastic wake as compared to the Newtonian wake ($\beta = 0.2$); the viscoelastic
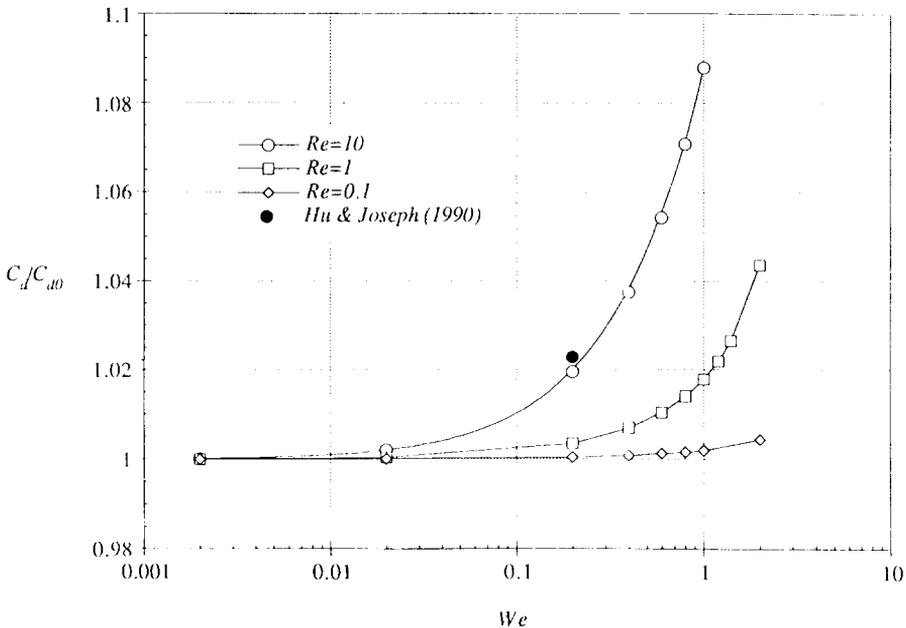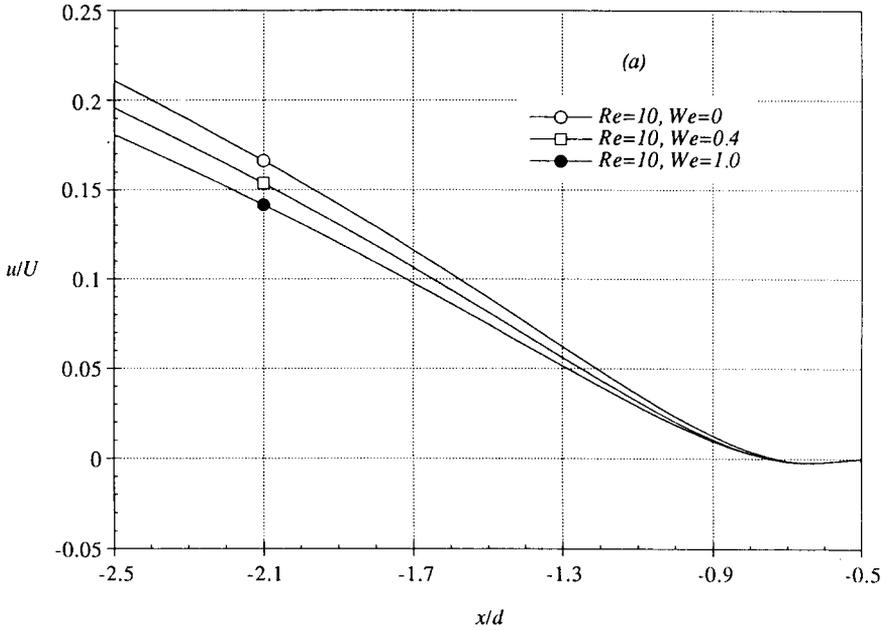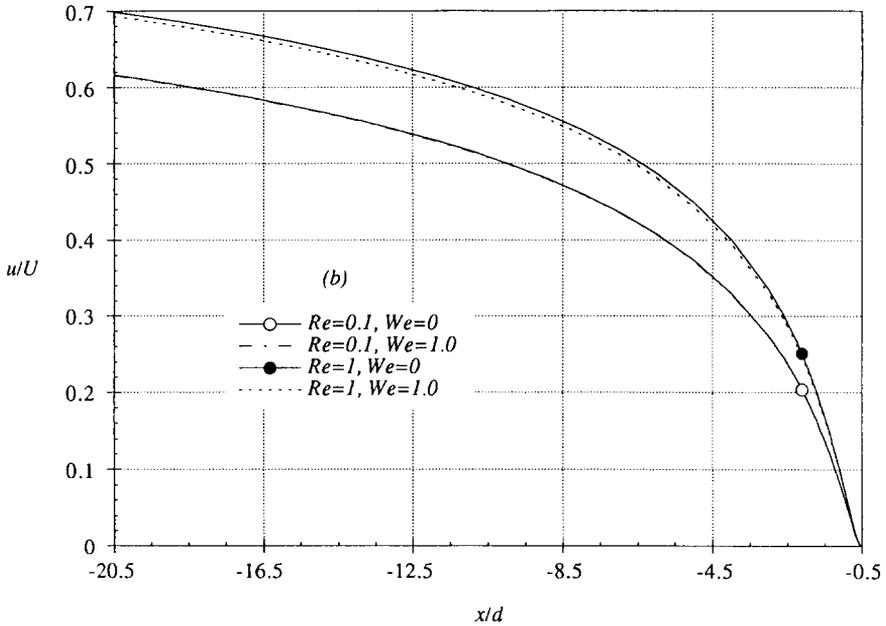

Fig. 6. The effect of Weissenberg number on the drag of a cylinder in an unbounded flow of an Oldroyd-B fluid. C_{d0} is the drag coefficient computed for a Newtonian fluid ($We = 0$). A data point of Hu and Joseph [18] for $Re = 10$ is also shown for comparison.

(a)

(b)

Fig. 7. The velocity distribution along the centerline of the wake of an unbounded viscoelastic flow field around a cylinder. (a) The wake is lengthened by elasticity. Also note the recirculation zone behind the cylinder $(-0.7 < x/d < -0.5)$ at $Re = 10$. (b) The elastic effect increases with Re. For $Re = 0.1$, the Newtonian and viscoelastic profiles are indistinguishable.

drag now falls below the Newtonian drag (Fig. 10(b)). For $\beta = 0.5$, the strongest blockage computed, there is an overshoot in the viscoelastic velocity profile, giving rise to a negative wake. In this case, the viscoelastic drag is considerably smaller than the Newtonian drag.

Somewhat surprisingly, the evolution of the viscoelastic wake is not completely smooth. From $\beta = 0.2$ to $\beta = 0.33$, the viscoelastic profile is not uniformly elevated with respect to the Newtonian profile. Instead, there appears a small region immediately behind the cylinder ($x/d \geqslant -1$) in which the viscoelastic fluid experiences a strong acceleration. After that, the velocity recovery is suppressed and the viscoelastic profile again beomes entirely above the Newtonian one. The computations for $\beta = 0.25$ and $\beta = 0.33$ have been double-checked using finer mesh, and the peculiar shape of the velocity profile stands.

This localized upstream shift in the streamlines was first noticed by Chilcott and Rallison [35]. Bush [38] confirmed the existence of this region by LDV measurements for the sphere-in-a-tube configuration using dilute polyacrylamide solutions in liquid glucose and water. He also employed numerical computations to examine the roles of wall confinement and constitutive models in this phenomenon. It was noted that the local acceleration is increased by wall proximity, which is consistent with our results, but he never obtained negative wake for β up to 0.5. His simulation also revealed an intriguing effect of the solvent. For a Maxwell model, this acceleration region does not appear. This probably explains why using a large
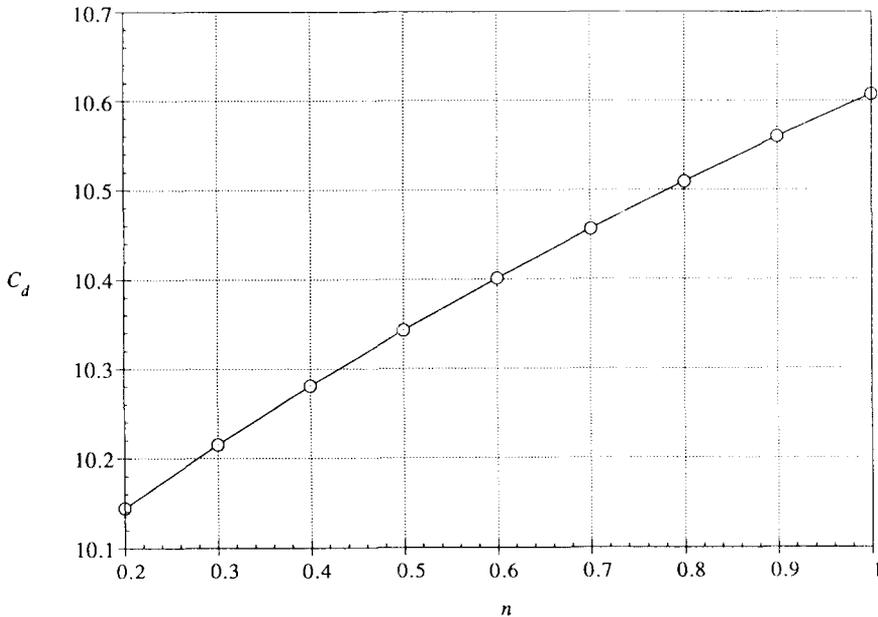

Fig. 8. The effect of shear thinning on the drag coefficient of a circular cylinder in an unbounded flow. $Re = 1$, $We = 1.0$.
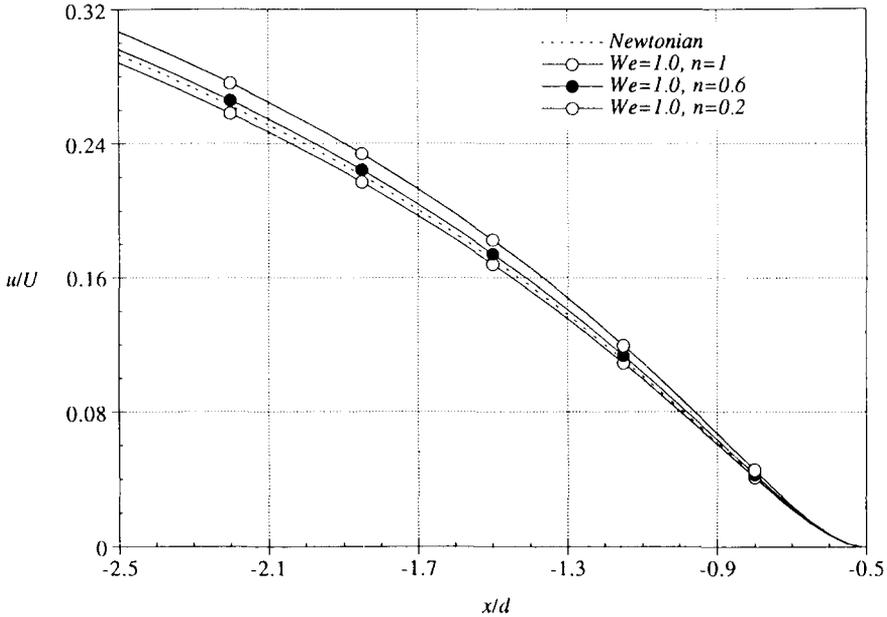
Fig. 9. Effect of shear thinning on the velocity distribution along the center line of an unbounded flow field around a cylinder. $Re = 1$.

retardation time ($\lambda_2/\lambda_1 = 0.6$ and 0.8) in the Oldroyd-B model, Bush [38] obtained a stronger localized upstream shift in the streamlines than we do. This phenomenon is not yet well understood and calls for more detailed research. For example, both Chilcott and Rallison [35] and Bush [38] computed inertialess flows and the effect of Re is not clear. Besides, we see this effect only in an intermediate range of β while Chilcott and Rallison observed it in an infinite domain.

The negative wake is another interesting issue. For spheres settling in a tube filled with quiescent polyox solutions, Sigli and Coutanceau [6] observed that the magnitude of the velocity overshoot in the wake increases with We and wall confinement, but decreases with Re. Zheng et al. [37] argued that the negative wake is a result of combined effects of shear thinning and viscoelasticity, because shear thinning is known to induce an upstream shift in the streamlines. Our results show that a negative wake may also occur for a two-dimensional flow past a cylinder when shear thinning is absent. The overshoot in Fig. 13 seems to be related to the wall proximity, which also tends to shorten the wake and shift streamlines upstream. The exact mechanism for the negative wake is not clear; it has been speculated that the negative wake may be associated with the strong elongational flow behind the solid obstacle [39]. Recently, Joseph and Feng [40] argued that normal stresses are responsible.

The effect of shear thinning in the bounded flow is similar to that in an unbounded flow: it tends to shorten the wake and shift the streamlines upstream. Fig. 14 shows this trend for $\beta = 0.33$. It is expected that shear thinning will enhance
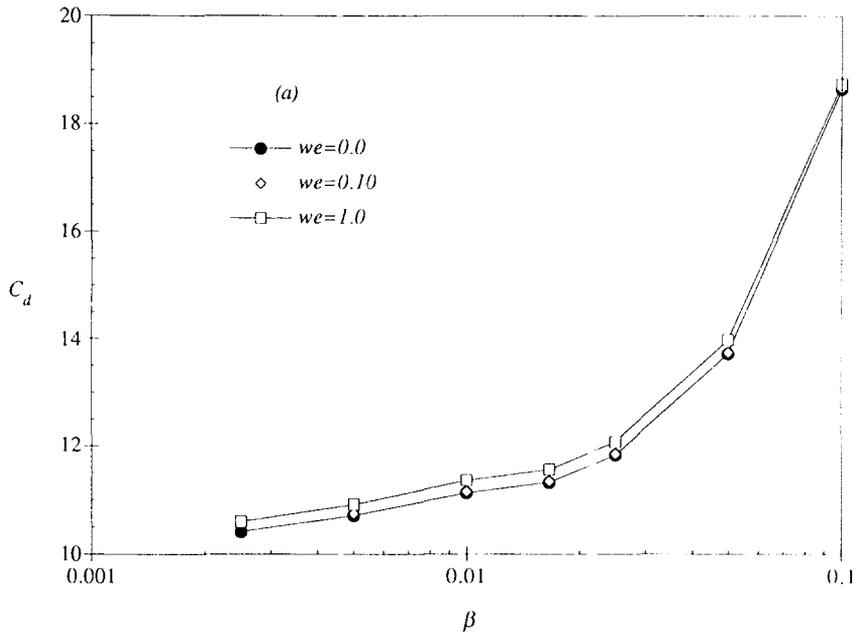
(a)
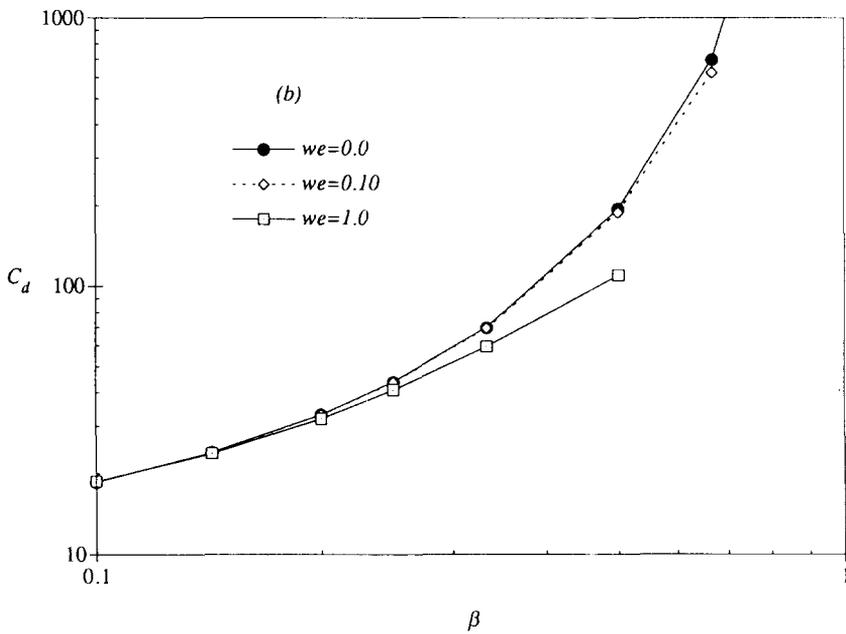
(b)

Fig. 10. Wall effects on the drag coefficient for a Newtonian fluid and an Oldroyd-B fluids at two Weissenberg numbers. $Re = 1$. The curves are plotted in two parts (a and b) to show details at low blockage.
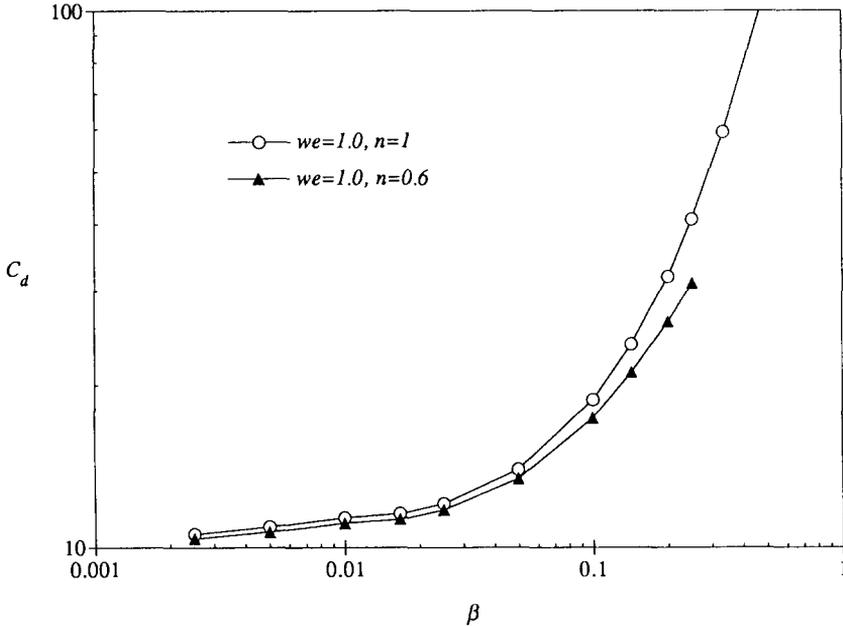
Fig. 11. Wall effects on the drag coefficient for viscoelastic fluids with or without shear thinning. $Re = 1$.

the overshoot for $\beta = 0.5$, but the combination of strong blockage and shear thinning renders numerical convergence impossible for this case.

4. Concluding remarks

The principal results of this paper can be summarized as follows:

(1) Effects of elasticity. For unbounded flows or flows with weak blockage ($\beta < 0.1$), elasticity increases the drag on the cylinder for all Reynolds numbers that we have tested. The wake is lengthened with a downstream shift of streamlines. For flows with stronger blockage ($\beta > 0.1$), the trend is completely reversed. The drag is decreased by elasticity and the wake is shortened.

(2) Effects of shear thinning. Shear thinning decreases the drag, shortens the wake and causes an upstream shift in streamlines. This is true for all Reynolds numbers, Weissenberg numbers and blockage ratios we have tested.

(3) Wall effects. Wall proximity shortens the wake and increases the drag for flows of Newtonian fluid and viscoelastic fluids with or without shear thinning. This effect is reduced by elasticity and shear thinning.

(4) A negative wake appears as a result of the combination of viscoelasticity and strong blockage. Shear thinning is believed to enhance the negative wake.

(5) A localized upstream shift of streamlines may occur in a small region behind the cylinder while the rest of the wake is extended. The mechanism of this effect is not clear.

The basic features of a two-dimensional flow around a cylinder in a channel are similar to those for an axisymmetric flow past a sphere in a tube. Recently, Brown and McKinley [41] recommended using the two-dimensional flow as a benchmark problem for numerical algorithms because it offers more convenience in experiments than its axisymmetric counterpart.

As mentioned before, this paper focuses on the drag coefficient of a cylinder and the velocity field in it wake. These are among the most basic characteristics of the flow. Recent experimental studies have already begun to explore more delicate aspects of the flow, such as instability of a steady flow past a cylinder [13] and arrays of cylinders [42]. These present new challenges to numerical simulations.
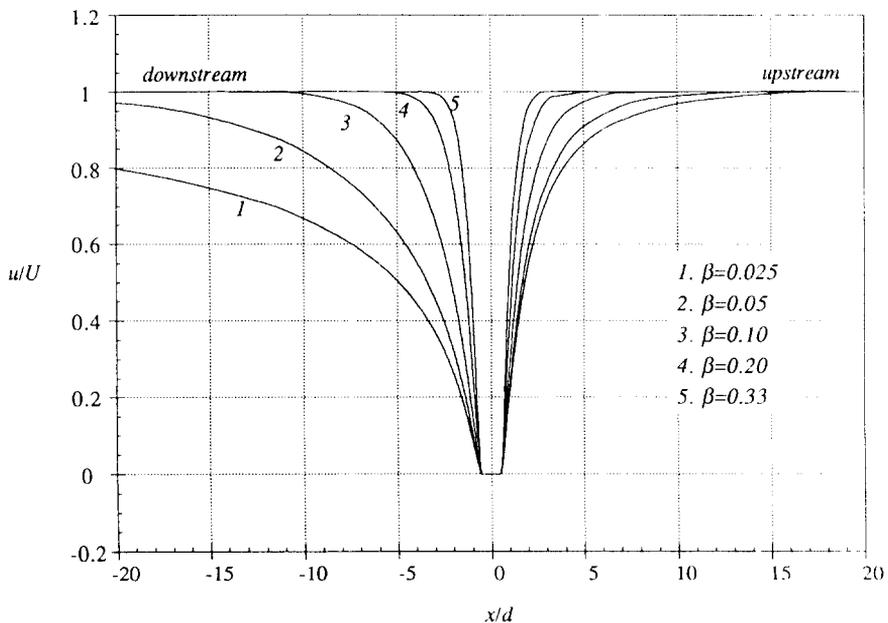
Acknowledgment

Fig. 12. Effects of blockage on the velocity distribution along the centerline of the channel. The fluid is viscoelastic without shear thinning. $Re = 1$, $We = 1$.
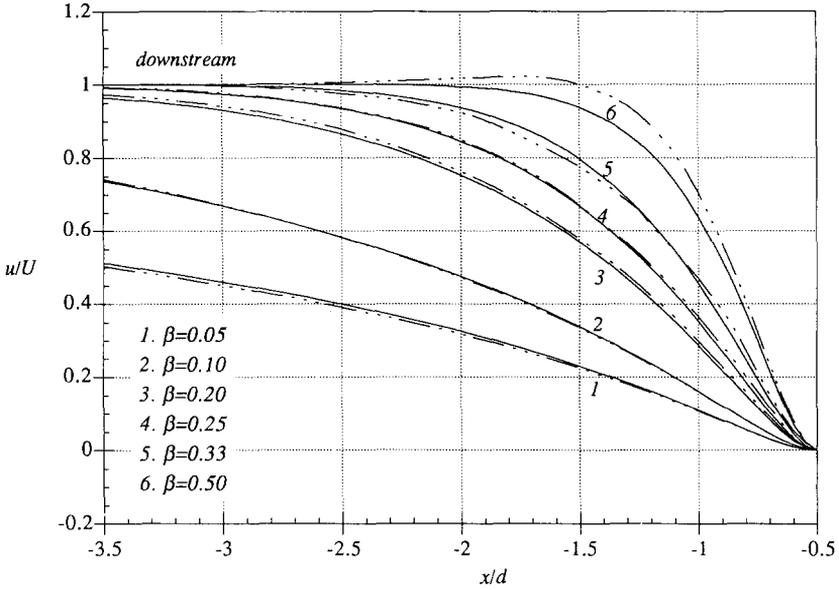
Fig. 13. Comparison of velocity distributions along the centerline of the wake at different blockage ratios. Solid lines represent Newtonian profiles at $Re = 1$; dashed lines represent profiles of an Oldroyd-B fluid at $Re = 1$ and $We = 1$.
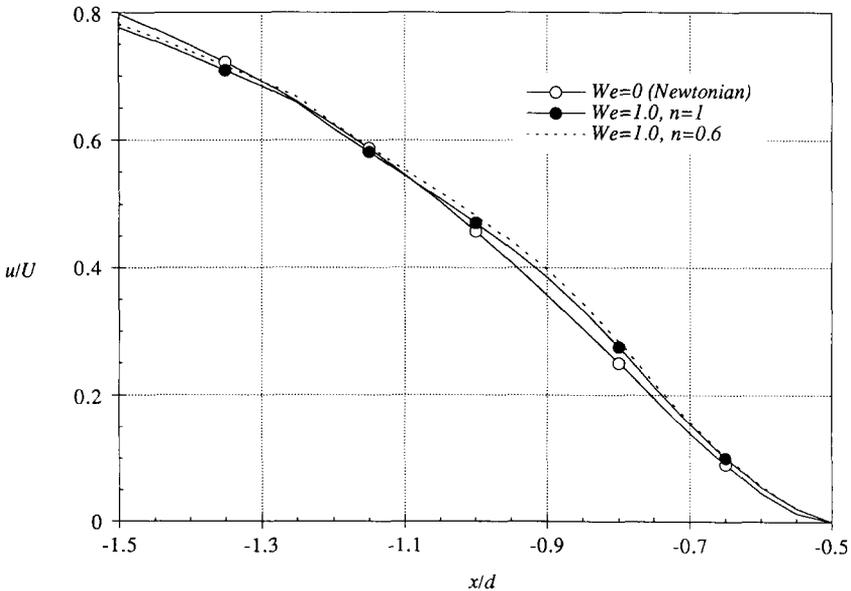

Fig. 14. Effects of shear thinning on the velocity distribution along the centerline of the channel. $Re = 1$, $\beta = 0.33$.

References

[1] K. Walters and R.I. Tanner, in P.R. Chhabra and D. De Kee (Eds.), The motion of a sphere through an elastic fluid, Transport Processes in Bubbles, Drops, and Particles, Hemisphere, 1992 pp. 73–86.

[2] C. Chmielewski, K.L. Nichols and K. Jayaraman, A comparison of the drag coefficients of spheres translating in corn-syrup-based and polybutene-based Boger fluids, J. Non-Newtonian Fluid Mech., 35 (1990) 37–49.

[3] B.H.A.A. van den Brule and G. Gheissary, Effects of fluid elasticity on the static and dynamic settling of a spherical particle, J. Non-Newtonian Fluid Mech., 46 (1993) 123–132.

[4] V. Tirtaatmadja, P.H.T. Uhlherr and T. Sridhar, Creeping motion of spheres in fluid M1, J. Non-Newtonian Fluid Mech., 35 (1990) 327–337.

[5] G.C. Georgiou and M.J. Crochet, The simultaneous use of 4×4 and 2×2 bilinear stress elements for viscoelastic flows, Comput. Mech., 22 (1993) 341–354.

[6] D. Sigli and M. Coutanceau, Effect of finite boundaries on the slow laminar isothermal flow of a viscoelastic fluid around a spherical obstacle, J. Non-Newtonion Fluid Mech., 2 (1977) 1–21.

[7] C. Bisgaard, Velocity fields around spheres and bubbles investigated by laser-Doppler anemometry, J. Non-Newtonian Fluid Mech., 12 (1983) 283–302.

[8] R.P. Chhabra and P.H.T. Uhlherr, The influence of fluid elasticity on wall effects for creeping sphere motion in cylindrical tubes, Can. J. Chem. Engng., 66 (1988) 154–157.

[9] B. Mena, O. Manero and L.G. Leal, The influence of rheological properties on the slow flow past spheres, J. Non-Newtonian Fluid Mech., 26 (1987) 247–275.

[10] O. Hassanger and C. Bisgaard, A Lagrangian finite element method for the simulation of flow of non-Newtonian liquids, J. Non-Newtonian Fluid Mech., 12 (1983) 153–164.

[11] R.P. Chhabra and P.H.T. Uhlherr, Wall effect for high Reynolds number motion of sphere in shear thinning fluid, Chem. Eng. Commun., 5 (1980) 115–124.

[12] W.M. Jones, A.H. Price and K. Walters, The motion of a sphere falling under gravity in a constant-viscosity elastic liquid, J. Non-Newtonian Fluid Mech., 53 (1994) 175–196.

[13] G.H. McKinley, R.C. Armstrong and R.A. Brown, The wake instability in viscoelastic flow past confined circular cylinders, Phil. Trans. R. Soc. London, A344 (1993) 265–304.

[14] D.D. Joseph, Fluid Dynamics of Viscoelastic Liquids, Springer-Verlag, 1990.

[15] D.F. James and A.J. Acosta, The laminar flow of dilute polymer solutions around circular cylinders, J. Fluid Mech., 42 (1970) 269–288.

[16] J.S. Ultman and M.M. Denn, Slow viscoelastic flow past submerged objects, Chem. Eng., 2 (1971) 81–89.

[17] V. Delvaux and M.J. Crochet, Numerical prediction of anomalous transport properties in viscoelastic flow, J. Non-Newtonian Fluid Mech., 37 (1990) 297–315.

[18] H.H. Hu and D.D. Joseph, Numerical simulations of viscoelastic flow past a cylinder, J. Non-Newtonian Fluid Mech., 37 (1990) 347–377.

[19] A. Konuita, P.M. Adler and J.M. Piau, Flow of dilute polymer solutions around circular cylinders, J. Non-Newtonian Fluid Mech., 7 (1980) 101–106.

[20] B. Mena and B. Caswell, Slow flow of an elastico-viscous fluid past an immersed body, Chem. Eng. J., 8 (1974) 125–134.

[21] P. Townsend, A numerical simulation of Newtonian and visco-elastic flow past stationary and rotating cylinders, J. Non-Newtonian Fluid Mech., 6 (1980) 219–243.

[22] J.M. Broadbent and B. Mena, Slow flow of an elastico-viscous fluid past cylinders and spheres, Chem. Eng. J., 8 (1974) 11–19.

[23] O. Manero and B. Mena, On the slow flow of viscoelastic liquids past a circular cylinder, J. Non-Newtonian Fluid Mech., 9 (1981) 379–287.

[24] R.L. Christiansen, A laser-Doppler anemometry study of viscoelastic flow past a rotating cylinder, Ind. Eng. Chem. Fundam., 24 (1985) 403–408.

[25] E.O.A. Carew and P. Townsend, Slow visco-elastic flow past a cylinder in a rectangular channel, Rheol. Acta, 30 (1991) 58–64.

[26] S.A. Dhahir and K. Walters, On non-Newtonian flow past a cylinder in a confined flow, J. Rheol., 33 (1989) 781–804.

[27] F.P.T. Baaijens, H.P.W. Baaijens, G.W.M. Peters and H.E.H. Meijer, An experimental and numerical investigation of a viscoelastic flow around a cylinder, J. Rheol., 38 (1994) 351–376.

[28] D. Rapajopalan, R.C. Armstrong and R.A. Brown, Finite element methods for calculation of steady, viscoelastic flow using constitutive equations with a Newtonian viscosity, J. Non-Newtonian Fluid Mech., 26 (1990) 159–192.

[29] V. Legat and J.-M. Marchal, On the stability and accuracy of fully coupled finite element techniques used to simulate the flow of differential viscoelastic fluids: a one-dimensional mode, J. Rheol., 36 (1992) 1325–1348.

[30] F. Debae, V. Legat and M.J. Crochet, Practical evaluation of four mixed finite element methods for viscoelastic flow, J. Rheol., 38 (1994) 421–442.

[31] J. Happel and H. Brenner, Low Reynolds number hydrodynamics, Noordhoff, Leiden 1973.

[32] A.S. Ramamurthy and C.P. Ng, Effect of blockage on steady force coefficients, J. Eng. Mech., (ASCE) 99 (1973) 755–772.

[33] J. Feng, H.H. Hu and D.D. Joseph, Direct simulation of initial value problems for the motion of solid bodies in a Newtonian fluid. Part 1. Sedimentation, J. Fluid Mech., 261 (1994a) 95–134.

[34] D. Sucker and H. Brauer, Fluiddynamik bie quer angeströmten zylindern, Wärme- unds Stoffüber-trag., 8 (1975) 149–158.

[35] M.D. Chilcott and J.M. Rallison, Creeping flow of dilute polymer soltuions past cylinders and spheres, J. Non-Newtonian Fluid Mech., 29 (1988) 381–432.

[36] R. Zheng, N. Phan-Thien and R.I. Tanner, On the flow past a sphere in a cylindrical tube: limiting Weissenberg number, J. Non-Newtonian Fluid Mech., 36 (1990) 27–49.

[37] R. Zheng, N. Phan-Thien and R.I. Tanner, The flow past a sphere in a cylindrical tube: effects of inertia, shear-thinning and elasticity, Rheol. Acta, 30 (1991) 499–510.

[38] M.B. Bush, The stagnation flow behind a sphere, J. Non-Newtonian Fluid Mech., 49 (1993) 103–122.

[39] M.B. Bush, On the stagnation flow behind a sphere in a shear-thinning viscoelastic liquid, J. Non-Newtonian Fluid Mech, 55 (1994) 229–247.

[40] D.D. Joseph and J. Feng, The negative wake in a second-order fluid, J. Non-Newtonian Fluid Mech., 57 (1995) 313–320.

[41] R.A. Brown and G.H. McKinley, Report on the VIIIth International Workshop on Numerical Methods in Viscoelastic Flows, J. Non-Newtonian Fluid Mech., 52 (1994) 407–413.

[42] C. Chmielewski and K. Jayaraman, Elastic instability in crossflow of polymer solutions through periodic arrays of cylinders, J. Non-Newtonian Fluid Mech., 48 (1993) 285–301.